EphA2 and Phosphoantigen-Mediated Selective Killing of Medulloblastoma by γδT Cells Preserves Neuronal and Stem Cell Integrity

Lola Boutin[1*], Mingzhi Liu[1], Julie Déchanet Merville[2], Oscar Bedoya-Reina[3,4], Margareta T Wilhelm[1*].

[1]Department of Microbiology, Tumor and Cell Biology (MTC), Karolinska Institutet, 171 77 Stockholm, Sweden.

[2]Bordeaux University, CNRS, ImmunoConcept, UMR 5164, 33000 Bordeaux, France.

[3] School of Medical Sciences, Örebro University, 70182 Örebro, Sweden.

[4]Department of Women's and Children's Health, Karolinska Institutet, 171 77 Stockholm, Sweden.

*Corresponding authors: margareta.wilhelm@ki.se, lola.boutin@ki.se

Abstract

Medulloblastoma (MB) is a pediatric brain tumor that develops in the cerebellum, representing one of the most common malignant brain cancers in children. Standard treatment includes surgery, chemotherapy, and radiation, but despite a 5-year survival rate of approximately 70%, these therapies often lead to significant neurological damage in the developing brain. This underscores the urgent need for less toxic, more effective therapeutic alternatives. Recent advancements in cancer immunotherapy, including immune checkpoint inhibitors and CAR-T cell therapy, have revolutionized cancer treatment. One promising avenue is the use of Gamma Delta (γδ)T cells, a unique T cell population with potential advantages such as non-alloreactivity, potent tumor cell lysis, and broad antigen recognition. However, their capacity to recognize and target MB cells remains underexplored. To investigate the therapeutic potential of γδT cells against MB, we analyzed the proportion and status of MB-infiltrated γδT cells within patient datasets. We next investigated the expression of γδT cell ligands on MB cells and identified EphA2 receptor and the phosphoantigen/Butyrophilin complex as key ligands, activating Vγ9Vδ1 and Vγ9Vδ2 T cells, respectively, leading to significant MB cell lysis in both monolayer and spheroid models. Importantly, preliminary safety data showed that γδT cells did not target differentiated neurons or neuroepithelial stem cells derived from induced pluripotent stem cells, underscoring the selectivity and safety of this approach. In conclusion, γδT cells trigger an efficient and specific killing of MB, and would offer a promising novel therapeutic strategy.

Key messages:

Medulloblastoma patients often experience significant long-term side effects from current standard treatments. Immunotherapy has emerged as a promising alternative to conventional therapeutic approaches. In our study, we demonstrated that γδT cells can efficiently and specifically target medulloblastoma cells without causing harm to healthy neuronal tissue. These findings suggest that γδ

34 T cell therapy may provide therapeutic benefits while potentially reducing treatment-related toxicity in
35 medulloblastoma patients.

36

37

Introduction

Medulloblastoma (MB), the most common malignant pediatric tumor of the central nervous system (CNS), accounting for 20% of all pediatric CNS tumors, represents a heterogeneous group of brain tumors usually found in cerebellum. Current treatment protocols have improved the 5-year-overall survival (5y-OS) rate to 80% globally[1]. Four main subgroups of MB have been identified by molecular classification: Wingless (WNT), Sonic Hedgehog (SHH), Group (Grp)3, and Group (Grp)4[2]. Prognosis is strongly linked to the MB subgroup, with WNT-activated MB having a more favorable outcome (90% 5y-OS) and Grp3, the less favorable (50% 5y-OS) with a high metastatic rate[3]. MB patients are treated according to a standard of care, which includes surgical resection, adjuvant chemotherapy and, in some cases, craniospinal irradiation. However, the treatment line often leads to systematic and irreversible neurological deficits, resulting in a decline in intellectual and cognitive function, due to damage of the healthy brain tissue[4]. Highlighting the importance of identifying less toxic and more effective therapeutic alternatives for MB.

Recently, immunotherapy has paved the way to propose more specific and safer alternatives to conventional chemotherapies. MB is known as a cold tumor with an immune evasive microenvironment, mostly limited to M2-like microglia and macrophage infiltration[5]. In addition, MB is characterized by a low mutation burden and the absence of PD-L1 expression, which correlates with low T cell infiltration[6]. While immune checkpoint-blockade (ICB) therapy (e.g. PD1/PD-L1, CTLA-4) has led to a major breakthrough for many solid tumors, MB does not seem to benefit from it[7]. Adoptive cell therapies such as CAR-T or NK cell therapy are currently being evaluated in various clinical trials for pediatric brain tumors including MB patients[8,9], with CAR-T cells targeting B7-H3, GD2, IL-13α, EphA2 or HER2 showing some promise[8]. However, tumor cells can escape CAR-T cells by downregulating the expression of the target molecules, as has been demonstrated in 30-70% of patients undergoing therapy[10].

γδT cells are a MHC-peptide unrestricted T cell population which recognizes conserved cellular stress patterns upregulated in infected and transformed cells[11]. They possess both adaptive and innate receptors such as a functional T cell receptor (TCR) associated with a CD3 molecule, as well as NKG2D and Toll-like receptors (TLR), which enable them to recognize a broad spectrum of ligands[12]. γδT cells express a TCR composed of Vγ and Vδ chains, the former defining the γδT subpopulation (Vδ1, Vδ2 and Vδ3), and the preferred location. Invariant Vγ9Vδ2 T cells are the main population in the peripheral blood system (>90% of total γδT) sensing phosphoantigen (pAgs) level dysregulation in transformed or infected cells, whereas Vδ1 and Vδ3 subpopulations are mainly present in tissues where they are involved in immune surveillance but also in the maintenance of tissue homeostasis[13].

Allogeneic therapies based on γδT cells have been shown to be clinically safe and effective in various cancers, demonstrating the potential of using an allogeneic γδT cell bank for tumor immunotherapy[14–

[16]. However, the ability of γδT cells to target and eliminate MB cells is poorly documented. Here, we show that both Vγ9Vδ1T and Vγ9Vδ2T cells can specifically eliminate MB cells without affecting healthy neural stem cells or neurons, highlighting the potential of using γδT cells for immunotherapy of medulloblastoma and other pediatric CNS tumors.

Materials & Methods

Deconvolution of bulk MB tumor samples and TIL abundance

Bulk RNA sequencing datasets were downloaded from GEO portal: Normal cerebellum (GSE44971) and MB patients (GSE37418 and GSE85217). Assessments of leucocyte fractions from the specified transcriptomes were performed by applying CIBERSORT (https://cibersort.stanford.edu/) with the matrix LM-7 as previously described[17,18]. Abundances were calculated from the CIBERSORT results and Sample Enrichment Score (SES). SES were computed by applying the open-source software AutoCompare-SES (https://sites.google.com/site/fredsoftwares/products/autocompare_ses) with normalized settings. Then, the open-source software DeepTIL (https://sites.google.com/site/fredsoftwares/products/deeptil) was used to automatically compute the abundance of the seven leucocyte subsets.

TCR repertoire analysis

To conduct the TCR repertoire analysis, we used the MB immune cell landscape dataset obtained by Riemondy et al. using single-cell sequencing[6]. Briefly, 29 samples were single-cell sequenced using 10X to a deep of 50,000 reads per cells, and processed using CellRanger and Seurat. The resulting dataset contains normalized expression for 4,669 MN tumor-infiltrating immune cells including clusters of microglia, myeloid, neutrophil, NK, T, and B cells. This data was downloaded from the pediatric Neuro-oncology Cell Atlas (pneuroonccellatlas.org) available at https://github.com/rnabioco/medulloblast on 08/09/2023. The available metadata from Supplementary Table 1 of Riemondy et al. was included in the analysis. To study the γδ repertoires in T cells of MB, BAM files from single-cell alignments of the 29 samples analyzed were obtained from the GEO SuperSeries accession number GSE156053 on 09/12/2023. These files were further processed with TRUST4, to determine the repertoires for each cell independently, following their barcodes[19].

T cell differentiation state analysis

To determine the differentiation state of T cells, gene signatures for 1) naïve, 2) resident, 3) pre-exhausted, 4) exhausted, and 5) effector-memory cells were generated **(Table S1)**. For each of these

106 gene lists a signature score was computed as the average expression of each reference gene sets, minus
107 the average of a (n) randomly selected set of genes (where n = max [# reference genes, 50]). The
108 signature score provides an estimation of the transcriptional resemblance of each cell to each reference
109 cluster of interest. Additionally, the normalized expression for each gene within these signatures was
110 obtained.

111

112 **Cell culture**

113 Neuroepithelial stem (NES) cells were obtained as previously described[20]. NES cells were cultured in
114 flasks coated with 20 µg/ml poly-L-ornithine (Sigma, P3655) and 1 µg/ml laminin (Sigma, L2020) in
115 complete neural stem cell medium (DMEM/F12+Glutamax (ThermoFisher, 31331093) supplemented
116 with 1% N2 supplement (ThermoFisher, 17502001), 0.1% B27 supplement (ThermoFisher, 17504044),
117 10 ng/ml FGF2 (Qkine, Qk053), 10 ng/ml EGF (PeproTech, AF100-15) and 1% penicillin-streptomycin
118 (Sigma, P4333)). For neuron differentiation, NES cells were seeded in flat bottom 96 well-plates coated
119 with 20 µg/ml poly-L-ornithine and 2 µg/ml laminin at a concentration of $15x10^3$ cells/well in complete
120 NES media. After 24 hours, NES media was removed and replaced with neuron differentiation media
121 (DMEM/F12+Glutamax with 1% N2 supplement, 0,1% B27 supplement and 1 µg/ml laminin). NES
122 cells were maintained in neuron differentiation media for a minimum of 3 weeks to ensure neuronal
123 differentiation.
124 CHLA-01-MED and CHLA-01R-MED cells were cultured in DMEM/F12+Glutamax with 20 ng/ml,
125 20 ng/ml EGF, 2% B27. DAOY and ONS-76 cells were maintained in DMEM (ThermoFisher,
126 41966052) supplemented with 10% FBS (Hyclone, SV30160.03HI). Additionally, medium for DAOY
127 cells contains 1% MEM non-essential amino acids, 1% HEPES, and 1% Glutamax (ThermoFisher, cat.
128 11140050, SH30237.01, and 35050061, respectively). UW228-3 cells were cultured in RPMI-
129 1640+Glutamax (ThermoFisher, 61870044) supplemented with 10% FBS. D425 and D458 cells were
130 cultured in DMEM/F12+Glutamax supplemented with 10% FBS. All cell lines tested negative for
131 mycoplasma and were authenticated by STR analysis at Eurofins (DAOY, D425, D458 CHLA-01-MED,
132 CHLA-01R-MED), or Multiplexion (ONS-76, UW228-3). Grp3-MB Patient-Derived Xenograft (PDX)
133 MB-LU-181 was established and cultured as described[21].
134 Jurkat JRT3 expressing Vγ9Vδ1-MAU TCR were obtained as described and cultured in RPMI-
135 1640+Glutamax supplemented with 10% FBS[22].
136

137 **Sorting and *ex-vivo* expansion of γδT cells**

138 Human peripheral blood mononuclear cells (PBMCs) were isolated from blood of healthy donors
139 obtained from Karolinska University Hospital (Stockholm, Sweden). PBMCs were collected by Ficoll
140 gradient centrifugation (Ficoll-Paque® PREMIUM, Cytiva, 17-5442-02) and resuspended in RPMI-

141 1640 medium supplemented with 10% heat-inactivated FBS. γδT cells were magnetically sorted using
142 EasySep™ Human Gamma/Delta T Cell Isolation Kit (Stemcell Technologies, 19255) according to the
143 manufacturer's protocol. Sorted fraction was expanded by activation with tetramer CD2/CD3/CD28
144 (Immunocult®, Stemcell Technologies, 10970) in ImmunoCult-XF T Cell Exp Medium (Stemcell
145 Technologies, 10981) supplemented with 300IU/ml recombinant human IL-2 (Stemcell Technologies,
146 78036) for 14 days. Expanded γδT cell purity was assessed by flow cytometry by staining with anti-
147 pan γδ TCR mAb and the expanded populations were kept for further experiments if γδT > 85%. After
148 expansion, γδT cells were maintained in ImmunoCult-XF T Cell Exp Medium supplemented with
149 300IU/ml recombinant human IL-2 for up to three weeks.

150

151 **Flow cytometry based-T cell activation**

152 For CD107a surface mobilization assays, target cells were treated for 18 hours with zoledronic acid
153 (Sigma, SML0223) in their maintenance media. Target cells were co-cultured for 4 hours with amplified
154 γδT cells (E/T ratio 1:1) in RPMI-1640 supplemented with 10% FBS containing Golgi Stop (BD
155 Biosciences, 554724) and anti-CD107a mAb for 4 hours. Cells were harvested and stained with anti-
156 pan γδ TCR, anti-Vδ2 and anti-Vδ1 mAbs. For CD69 expression, target cells were co-cultured with
157 JRT3-MAU cells (E/T ratio 1:1) in RPMI-1640 supplemented with 10% FBS for 4 hours. Cells were
158 harvested and stained with anti-Vδ1 and anti-CD69 mAbs. Flow cytometry data were acquired using
159 BDCanto II cytometer (BD Biosciences) and analyzed using FlowJo v.10 software (Treestar).

160

161 **Flow cytometry staining**

162 All antibodies used for flow cytometry assays are described in supplemental materials.

163

164 **LDH-release cytotoxicity assay**

165 For monolayer killing assay, targets cells were seeded in flat-bottom 96-well plates in their maintenance
166 media one day prior to co-culture. For spheroid killing assay, target cells were seeded in U-bottom 96-
167 well low adherence plates (BRANDplates®, inertGrade™) 4 days prior co-culture in NES media. Target
168 cells were treated for 18 hours with zoledronic acid, followed by co-culture with amplified γδT cells
169 (E/T ratio 10:1) in RPMI-1640 supplemented with 5% Human serum (Sigma, H5667) for 8 hours.
170 Supernatants were collected and used for LDH (lactate dehydrogenase) measurement using CytoTox
171 96® kit (Promega, G1780) according to the manufacturer's protocol, and quantified by FLUOstar
172 Omega plate reader (Absorbance 490nm, BMG labtech). The percentage of target cell lysis was
173 calculated as follows: ((experimental release - spontaneous release)/ (maximum release - spontaneous

174 release)) × 100. Spontaneous and maximum release values were determined by adding either medium
175 or lysis buffer (provided in the kit) to target cells without T cells. For NKG2D blocking assay, 10 µg/mL
176 of anti-NKG2D mAb was added to the γδ T cells 20 minutes prior co-coculture and kept throughout the
177 experiment.
178
179 **Statistical analysis**
180 Samples collected from anonymized healthy human donors have been used in this study. Data were
181 analyzed with GraphPad Prism software v.10.1.2 and are presented as mean ± SD; or survival curve.
182 Statistical analysis data was performed by unpaired nonparametric t-student test; log-rank test; or by
183 two- and one-way ANOVA followed by Tukey, Sidák, or two-tailed Dunnett's tests to correct for
184 multiplicity. *P*-values below 0.05 were considered statistically significant.
185
186
187 **Results**
188 **γδT cells are predicted to be present in healthy cerebellum and in MB tumors.**
189 The presence of γδT cells in healthy CNS and in CNS tumors has been poorly reported. Moreover, the
190 difficulty of transcriptionally separating γδT from $CD8^+$ αβT and NK cells makes it difficult to predict
191 their proportion from tissue or tumor mRNA samples[23]. Recently, an updated version of an
192 immunosignature (LM-7) CIBERSORT deconvolution matrix optimized for γδT cells was developed[17].
193 Using the LM-7 matrix, we estimated the immune infiltration, comparing healthy cerebellum from five
194 fetal and four adult tissues (GSE44971) with 76 MB patients (GSE37418). As previously described, we
195 found that the immune landscape of MB is not different from that of non-tumoral tissue (**fig.1A**, **Table**
196 **S2**)[24]. In particular, we found no significant differences in the proportion of different immune cell
197 populations between fetal/adult cerebellum and MB (two-side Kruskal-Wallis, $p>0.05$) for the
198 predictions of CIBERSORT and SES+CIBERSORT, with the solely exception of $CD4^+$ T cells that
199 present a marginal significant difference between fetal and malignant tissues (two-side Mann-Whitney
200 U, $p=0.013$) for the CIBERSORT prediction (**Fig. S1A**). The abundance value was similar to previous
201 reports in which MB had the lowest immune cell abundance of all tumors, including other brain tumors
202 such as ependymoma (7.43), glioblastoma (15.75) or pilocytic astrocytoma (22.29), making MB one of
203 the most immune-evasive tumors[17].
204 To further analyze the differences in immune cell infiltration, and specifically γδT cell infiltration
205 between the different MB subgroups, we used a larger MB patient cohort (GSE85217, 763 patients)[3].
206 We observed some differences in immune cell infiltration between the subgroups, with SHH-MB having
207 an increased fraction of myeloid cells and a lower proportion of granulocytes compared to other
208 subgroups, consistent with previous findings (**fig.1B**, **Table.S3**)[25]. The ratio of myeloid cells to T cells
209 is also significantly higher in SHH-MB (**Fig. S1B)**. $CD4^+$ T cells are the major lymphoid subsets in MB,

210 followed by γδT cells. In contrast, $CD8^+$T cells and NK cells, two cytotoxic subsets, are found in very
211 low abundance in the tumor.
212 Interestingly, the frequency of γδT cells in MB differs between the subgroups, with the highest score in
213 Grp4-MB (**fig.1C**), while αβT cells ($CD8^+$ and $CD4^+$) are more homogeneously distributed in the
214 subgroups (**fig.1D**). In addition, the four MB subgroups can be further divided into 12 subtypes
215 according to age, histology, methylation profile and driver mutations[3], and the abundance score of γδT
216 cells varies between subtypes in the same subgroup, except for WNT-MB (**fig.1E)**. We observed an
217 increase of γδT cell score in SHHγ and Grp4γ and a slight decrease in Grp3γ subtypes. γδT cell
218 infiltration in many tumor types have been shown to be associated with a favorable outcome[26,27]. We
219 investigated whether the γδT cell scores correlate with prognosis in MB. Using the same cohort, patients
220 were divided into γδT cell high vs γδT cell low abundance score (1st vs 4th quartile), but we found no
221 significant correlation between γδT cell frequency and survival (p= 0.6570, log-rank test, **fig.1F).** In
222 conclusion, we show here that γδT cell infiltration is predicted for normal cerebellum and MB, with
223 some differences between the different MB subgroups and subtypes, but γδT cell frequency did not
224 correlate with prognosis, possibly due to its global low frequency.
225
226 **Tumor infiltrated γδT cells show a tissue resident phenotype.**
227 To further characterize the phenotype and activation state of γδT cells in MB, we extracted the
228 BCR/TCR repertoire using the Trust4 algorithm from a single-cell RNA dataset of 28 MB patients
229 (GSE155446, 1 WNT, 9 SHH, 7 Grp3 and 11 Grp4)[19]. Unfortunately, the number of B and T cells
230 recovered by the algorithm was low compared to the clustering shown in the pediatric neuro-oncologic
231 cell atlas. In total, 21 B cells, 56 αβT cells and 52 γδT cells were identified by the algorithm with a
232 complete or partial BCR/TCR identification (**Table.S4**). Interestingly the γ- and the β-VJC segments
233 were recovered better than their δ- and α- pairs. Therefore, we focused our analysis of γδT-infiltrated
234 cells on the γ-chain. Analysis of the variable (V)γ-segment repertoire revealed a high diversity with a
235 dominance for recombination of *TRGV2*, *TRGV9* and *TRGV10* genes in all MB subgroups (**fig.2A**).
236 *TRGV10* is characterized as a pseudogene (Vγ type III) and result in a non-functional γδTCR[28]. In
237 addition, *TRGV2, TRGV4* and *TRGV8,* already identified as brain-specific γδTCR signatures[29], were
238 present in MB. Interestingly, the public *TRGV9* clonotype (CALWEVQELGKKIKVF), which is present
239 in the blood from fetal to adult life, was detected in one MB patient[30]. We next compared the diversity
240 of the TRGV and TRGJ repertoires in the different MB subgroups (**fig.2B**). Grp3-infiltrated γδT cells
241 showed a significant reduction in TRGV and TRGJ diversity compared to the SHH and Grp4 MB and
242 had the highest proportion of non-functional $TRGV10^+$ cells. However, the CDR3 length distribution of
243 Grp3-infiltrated γδT cells is greater than in the other subgroups (Δ9 vs Δ6 or Δ7 amino acids for SHH-
244 and Grp4-MB, respectively) (**fig.2C**). Overall, analysis of the γδTCR repertoire revealed no specific
245 clonal expansion, suggesting a lack of tumor-specific reactivity.
246

247 To confirm this hypothesis, we examined the differentiation status of γδT and αβT cells identified by
248 the Trust4 algorithm, independent of MB subgroup. We compared gene expression profile specific to
249 naïve, effector memory, resident memory, pre-exhausted and exhausted T cells. There were few
250 differences between infiltrated γδT and αβT cells, which preferentially expressed *ILR7*, *CCL5*, *GZMK*,
251 *GZMA* and *CD69* (**fig.2D**). Evaluation of T cell differentiation state gene signatures of the T cell
252 differentiation state revealed a phenotype enriched with resident memory cells that neither proliferate
253 (*KI67*^{low}), show proinflammatory activity (*IFNG*^{low}), nor exhibit chronic activation-induced exhaustion
254 (**fig.2E)**. In summary, γδ T-infiltrated cells in MB do not express markers that would suggest active
255 involvement in anti-tumor immunity in MB.
256
257
258 **MB cells express γδT activating receptor ligands.**
259 Our analysis suggests that γδT cells infiltrate MB tumors but are insufficient in number and not
260 functionally active. However, one of the main advantages of γδT cells is that they allow for allogeneic
261 therapy due to their HLA-unrestricted activation. Therefore, we investigated which known ligands of
262 human γδTCRs or co-receptors are expressed by MB cells to identify a γδT cell subset that could target
263 MB cells. We examined a panel of seven MB cell lines covering three of the four MB subgroups (WNT
264 excluded) with two paired primary (P) and recurrent (R) tumors for Grp3 and Grp4-MB, and that are
265 considered relevant *in vitro* models[31]. We stained for γδTCR ligands: CD1d, CD1c, Ephrin Type-A
266 receptor 2 (EphA2) and Annexin A2 (ANXA2); NKG2D ligands: UL16 binding protein (ULBP)2/5/6;
267 MHC class I chain related protein (MIC)A/B; and DNAM-1 (CD226) ligands: CD112 and CD155 (**fig.3,**
268 **fig.S2**). Flow cytometry results showed that all MB cell lines were negative for CD1c and that only
269 DAOY cells presented weak expression of CD1d, as previously reported[32]. Overall, lipid presentation
270 by CD1 molecules does not appear to be a promising target candidate for MB.
271 However, all MB cell lines express EphA2 and ANXA2, specific ligands for Vγ9Vδ1 and Vγ8Vδ3T
272 cells, respectively[22,33]. CD112 and CD155, ligands of DNAM-1 an adhesion molecule, are also
273 expressed by all MB cell lines tested. Binding of DNAM-1 promotes activation of T/NK cells and
274 cytolytic degranulation[34]. However, CD112 and CD155 are also ligands for the checkpoint inhibitor
275 TIGIT, which could promote immunosuppression. Interestingly, only the SHH-MB cell lines (DAOY,
276 UW228-3 and ONS-76) were found expressing NKG2D ligands, suggesting that the immunogenicity of
277 Grp3 and Grp4-MB for the activation of NK and γδT cells may be reduced. In summary, we identified
278 a γδT cell ligand signature in MB cells that is subgroup-dependent, guiding to which γδT cell subset that
279 can target MB cells.
280
281 **EphA2-expressing MB cells trigger Vγ9Vδ1 T cell activation.**
282 EphA2 is a member of the Ephrin receptors, the largest receptor tyrosine kinase receptor family, and is
283 involved in several biological processes such as neuronal development, cytoskeleton dynamic,

284 migration, cell proliferation and angiogenesis. It is found to be overexpressed in tumors compared to
285 normal tissues, making it a good target for cancer therapy[35], which is supported by the development of
286 CAR-T cells targeting EphA2 for Grp3-MB and ependymoma[36]. As proof-of-principal for EphA2 as a
287 target ligand for Vγ9Vδ1T cells in MB, we used the Jurkat lymphoblastic cell line JRT3 (β-TCR chain
288 defective), engineered to express the Vγ9Vδ1-MAU TCR that was previously shown to recognize
289 EphA2[22]. The JRT3 model lacks cytotoxic capabilities but can be used to assess Vγ9Vδ1T cell
290 activation. We co-cultured JRT3-MAU with MB cell lines or with healthy iPSC-derived neuroepithelial
291 stem (NES) cells and measured the expression of the activation marker CD69 on JRT3-MAU by flow
292 cytometry. Co-culture with MB cell lines induced expression of CD69, regardless of MB subgroup,
293 resulting in strong activation of JRT3-MAU cells, except for the relapse cell line CHLA-01R-MED,
294 which showed a lower response (**fig.4A**). However, co-culture with non-cancerous healthy NES cells
295 resulted in significantly less activation of JRT3-MAU (**fig.4A**). Interestingly, the expression level of
296 EphA2 does not seem to correlate with the activation potential. To confirm this observation, we
297 measured EphA2 expression in NES cells, which was in the same range as in the D425 cell line but
298 activated JRT3-MAU to a much lower extent (**fig.3, fig.4B**). These results suggest the presence of
299 accessory signals on tumor cells that potentiate JRT3-MAU activation in addition to EphA2.
300
301 Next, we examined EphA2 RNA expression in both healthy cerebellum and MB patients using a publicly
302 available dataset[37] and found that the *EPHA2* gene expression is upregulated in WNT- and Grp3-MB
303 compared to normal cerebellum (**fig.4C**). To demonstrate the potential of Vγ9Vδ1T cells targeting Grp3-
304 MB, we co-cultured JRT3-MAU with the Grp3-MB PDX MB-LU-181, using D425 cells as a reference.
305 Results showed that JRT3-MAU upregulate CD69 expression in the presence of Grp3-MB PDX, yet to
306 a lesser extent than with the D425 cell line (**fig.4D**). Overall, these results confirmed the potential of
307 targeting EphA2-positive MB cells with Vγ9Vδ1T cells in a tumor-specific manner.
308
309
310
311 **Amino Bisphosphonates sensitize MB cells, but not healthy neuronal cells to Vγ9Vδ2T lysis.**
312 Cancer cells have a dysregulated metabolism with increased protein and lipid synthesis. Cholesterol, an
313 essential component of the cell membrane, is produced via the mevalonate synthesis pathways. One of
314 the intermediates of this pathway, isopentenyl pyrophosphate (IPP), can bind to the intracellular domain
315 of a member of the butyrophilin family, BTN3A1, and trigger the activation of Vγ9Vδ2T cells[38,39].
316 Vγ9Vδ2T cells are a peripheral population and are thought to naturally recognize and lyse leukemia
317 cells[40]. However, solid tumors often remain undetectable to Vγ9Vδ2T cell targeting[41]. Fortunately,
318 amino-bisphosphonate (NBP) molecules such as Zoledronate (zol) can increase intracellular IPP levels
319 by inhibiting the farnesyl diphosphate synthase in target cells, which then enhance Vγ9Vδ2T cell
320 recognition and activation (**fig.5A**).

321

322 BTN3A1 is ubiquitously expressed in all human cells, including healthy brain and MB cells. We tested
323 whether Vγ9Vδ2T cells can naturally recognize MB cells or be sensitized by zol treatment. NES and
324 MB cells were treated overnight with 0, 1 or 10µM of zol followed by co-culture with ex-vivo expanded
325 peripheral γδT cells isolated from healthy donors, the majority of which consisted of $V\delta2^+$ γδT cells
326 (**fig.5B**). The expression of the degranulation marker CD107a was analyzed on $V\delta2^+$ γδT cells by flow
327 cytometry. As expected, untreated NES and MB cells did not trigger Vγ9Vδ2T cell degranulation
328 (**fig.5C**). However, MB cells treated with 10µM zol, but not NES cells, were able to significantly
329 activate Vγ9Vδ2T cells. The suboptimal dose of 1µM showed a difference in the sensitivity of each cell
330 line to zol-treatment, with SHH cell lines and D425 cells inducing CD107a expression on Vγ9Vδ2T
331 cells, but not D458 and Grp4-MB cells. Furthermore, we detected differences between donors in terms
332 of zol-mediated activation against MB.
333 Next, we investigated whether zol treatment was sufficient to induce killing of MB cells by Vγ9Vδ2T
334 cells. We cultured MB cells, either as adherent monolayer (m) or as spheroids (sph), together with ex
335 vivo expanded γδT cells and quantified LDH release as a measure of cell death. LDH release results
336 showed that SHH-MB treated with zol induced killing by γδT cells in both monolayer and spheroid
337 conditions (**fig.5D)**. The cytotoxic potential of γδT cells against zol-treated SHH-MB cells is donor- and
338 target-dependent. Interestingly, the UW228-3 and ONS-76 cell lines are eliminated more efficiently in
339 spheroid form. We hypothesized that the percentage of killing in monolayer could be underestimated by
340 the readout method, as brightfield images taken after co-culture showed no remaining adherent MB cells
341 (**fig.S3**). Considering that we found that SHH-MB cells express NKG2D ligands, we further
342 hypothesized that NKG2D might act in synergy with TCR activation against SHH-MB. However,
343 NKG2D blocking on γδT cell did not affect the killing potential of zol-treated SHH-MB (**fig.5E, fig.S3**).
344 The CD107a results indicated that Grp3- and Grp4-MB were less sensitive to zol treatment, so the zol
345 concentration was increased to 50µM. Since Grp3- and Grp4-MB are naturally suspension cell types,
346 the treatment and co-culture were performed accordingly. Zol-treated D425 reached an average of 80%
347 of lysis, while the other three cell lines are closer to 45% (**fig.5F**). The Grp4-MB cell lines CHLA-01
348 and CHLA-01R grow as large neurospheres and have a lower proliferation rate than the Grp3 cells,
349 which could explain the difference. However, the difference between the D425 and D458 cell lines could
350 be the result of resistance acquired at relapse.
351

352 Finally, we examined the off-target effect of zol treatment on both proliferating NES cells and post-
353 mitotic neurons. We treated the neuronal cells both as monolayer and as spheroids with high doses of
354 zol (50 µM). The co-culture of zol-treated NES cells and neurons did not induce significant cytotoxicity-
355 mediated by Vγ9Vδ2T cells, demonstrating that zol treatment trigger specific targeting and killing of
356 MB cells by Vγ9Vδ2T cells while sparing healthy stem and differentiated neuronal cells (**fig.5G)**.
357

358 **Discussion**

359 CNS tumors remain among the most challenging to cure due to the complexity of the surrounding
360 environment. Brain cells are very sensitive to conventional cancer therapy such as chemotherapies and
361 radiotherapies[42], which has a significant impact on treatment outcomes and the long-term quality of life
362 of survivors. Given that MB develops in the cerebellum, which controls physical movements, balance,
363 and coordination[43], it is crucial to develop less toxic therapies to preserve these important bodily
364 functions.

365 A healthy immune system can distinguish between normal cells and infected or transformed cells. In
366 cancer patients, however, the immune system is often impaired. Therefore, allogeneic transfer of
367 immune cells from healthy individuals is a promising therapeutic strategy for cancer patients[44,45]. Non-
368 alloreactive and highly cytotoxic, γδT cells are a promising approach for allogeneic cell therapy in
369 cancer patients[46]. Here, we demonstrate that MB patients may benefit from allogeneic γδT cell transfer.
370 We confirm previous studies that the MB microenvironment lacks sufficient functional cytotoxic T cells,
371 including both αβT and γδT cells, to elicit a sufficient anti-tumor response from autologous T cells. The
372 small numbers of αβT and γδT cells identified by the TCR repertoire algorithm Trust4 showed no
373 significant clonal expansion or expression of activation/exhaustion markers, suggesting that
374 conventional ICB therapy may show limited efficacy in MB patients[47]. However, the low TCR recovery
375 could be due to insufficient sequencing quality or depth. Future sequencing experiments with fresh
376 patient samples and protocols optimized for TCR chain repertoire analysis could provide better insights.
377 B7-H3 is the only immune checkpoint protein reported to be significantly expressed in MB and other
378 brain tumors[48]. Strategies to use CAR-T cells targeting B7-H3 or antibody-drug conjugate are currently
379 being investigated in various brain tumors and show some therapeutic efficacy and promising safety
380 profile[49,50]. B7-H3 has been reported to confer resistance to killing by Vγ9Vδ2 T cells in a colon cancer
381 model in a STAT3/ULBP2 axis-dependent manner[51]. However, the direct or indirect effects of B7-H3
382 expressed by MB on the cytotoxicity of γδT cells remains to be investigated.

383

384 We showed that MB cells express several ligands recognized by different γδTCR receptors and co-
385 receptors (NKG2D and DNAM1), indicating the potential to target them with the corresponding γδT
386 cell subset. We tested the activation potential of different γδT cell subsets against MB cell lines based
387 on the TCR ligands they expressed. First, we demonstrated that seven MB cell lines and one PDX
388 expressed EphA2 and activated Vγ9Vδ1-MAU TCR Jurkat cells. Similarly, CAR-T cells targeting
389 EphA2 have shown strong anti-tumor potential in an *in vivo* Grp3-PDX model[36]. However, these CAR-
390 T cells lack the multipotency of multiple activating receptors expressed by γδT cells, which is an
391 advantage in heterogeneous solid tumors. On the other hand, maintaining and expanding T cell clones
392 in culture is challenging, so using the natural MAU clone may not be a viable therapeutic option. An
393 alternative is TCR-engineered T cell therapy, where the Vγ9Vδ1 TCR may be integrated into adoptive
394 cell therapy (ACT) candidates, such as γδT or NKT cells. The latter are particularly interesting as they

retain their endogenous TCR and can present dual-TCR recognition[52]. Additionally, zol treatment can sensitize MB cells to killing by *ex vivo* expanded Vγ9Vδ2T cells. Zol, commercially available as Zometa®, is prescribed for bone diseases, including bone malignancies and osteoporosis. We demonstrated the direct anti-tumor potential of zol against MB cells, however, it has also been reported that zol can inhibit pro-tumoral macrophages and microglia in a breast cancer brain metastasis model[53]. Importantly, both Vγ9Vδ1 and Vγ9Vδ2 T cell activation and killing were restricted to tumor cells, as normal NES and differentiated neurons did not triggering γδT cell activation, demonstrating the specificity of tumor cell targeting.

T cell-based therapies, including CAR-T cells and T cell engagers (TCE), face safety concerns, particularly regarding immune effector cell-associated neurotoxicity syndrome (ICANS) and cytokine storm syndrome (CSS)[54]. However, the first clinical trial of allogeneic intravenous Vγ9Vδ2 T cell transfer for solid tumors did not report severe side effects associated with the ACT[14]. Nevertheless, there is currently no clinical data on the safety of intraventricular infusion of allogeneic γδT cells in patients, making it essential to identify potential side effects associated with this therapeutic strategy. A phase II clinical study using autologous Vγ9Vδ2 T cells genetically modified to resist Temozolomide, a conventional chemotherapy used for glioblastoma, is ongoing and could provide future indication regarding the safety of intracranial injection of γδT cells (NCT05664243).

In conclusion, our study is the first to support the therapeutic potential of allogeneic γδT cells for MB patients and their potential as a safer alternative to conventional treatment.

Author contributions

Conception and design of the study: L.B and M.W.; Analysis and interpretation of the data: L.B. Generation and acquisition of data: L.B, M.L, O.B-R. Contribution of new reagents: J.D.M. Statistical analysis: L.B and O.B-R. Writing original draft of manuscript: L.B, O.B-R. J.D.M. and M.W, All authors have reviewed, read, and approved the submitted version of the manuscript.

Conflict of interest

The authors declare no financial or commercial conflict of interest.

Fundings

Cancerfonden (22 2236 Pj), Barncancerfonden (PR2021-0080 (MW), TJ2021-0137 and PR2021-0129 (O.C.B-R)), Radiumhemmets Forskningsfonder (#214173), and Vetenskapsrådet (2020-1427, 2023-02206). KI Forskningsbidrag grant 2022-01925 (O.C.B-R).

Data Availability Statement

All data relevant to the study are included in the article or uploaded as supplementary information

Acknowledgements

The authors thank the Biomedicum Flow Cytometry facility (BFC) for technical assistance. Part of the computations and data handling were enabled by resources provided by the National Academic Infrastructure for Supercomputing in Sweden (NAISS), partially funded by the Swedish Research Council through grant agreement no. 2022-06725. We thank everyone in the Wilhelm lab for technical assistance and helpful discussions.

References

1. Packer, R. J. *et al.* Phase III Study of Craniospinal Radiation Therapy Followed by Adjuvant Chemotherapy for Newly Diagnosed Average-Risk Medulloblastoma. *JCO* **24**, 4202–4208 (2006).
2. Taylor, M. D. *et al.* Molecular subgroups of medulloblastoma: the current consensus. *Acta Neuropathol* **123**, 465–472 (2012).
3. Cavalli, F. M. G. *et al.* Intertumoral Heterogeneity within Medulloblastoma Subgroups. *Cancer Cell* **31**, 737-754.e6 (2017).
4. Mulhern, R. K. *et al.* Neurocognitive Consequences of Risk-Adapted Therapy for Childhood Medulloblastoma. *JCO* **23**, 5511–5519 (2005).
5. Diao, S., Gu, C., Zhang, H. & Yu, C. Immune cell infiltration and cytokine secretion analysis reveal a non-inflammatory microenvironment of medulloblastoma. *Oncology Letters* **20**, 1–1 (2020).
6. Riemondy, K. A. *et al.* Neoplastic and immune single cell transcriptomics define subgroup-specific intra-tumoral heterogeneity of childhood medulloblastoma. *Neuro Oncol* noab135 (2021) doi:10.1093/neuonc/noab135.
7. Vermeulen, J. F. *et al.* Prognostic relevance of tumor-infiltrating lymphocytes and immune checkpoints in pediatric medulloblastoma. *Oncoimmunology* **7**, e1398877 (2018).
8. Schakelaar, M. Y. *et al.* Cellular immunotherapy for medulloblastoma. *Neuro-Oncology* **25**, 617–627 (2023).
9. Khatua, S. *et al.* Phase I study of intraventricular infusions of autologous ex vivo expanded NK cells in children with recurrent medulloblastoma and ependymoma. *Neuro Oncol* **22**, 1214–1225 (2020).
10. Mishra, A., Maiti, R., Mohan, P. & Gupta, P. Antigen loss following CAR-T cell therapy: Mechanisms, implications, and potential solutions. *Eur J Haematol* **112**, 211–222 (2024).
11. Hayday, A. C. [gamma][delta] cells: a right time and a right place for a conserved third way of protection. *Annu Rev Immunol* **18**, 975–1026 (2000).
12. Willcox, B. E. & Willcox, C. R. γδ TCR ligands: the quest to solve a 500-million-year-old mystery. *Nat Immunol* **20**, 121–128 (2019).
13. Chien, Y., Meyer, C. & Bonneville, M. γδ T cells: first line of defense and beyond. *Annu Rev Immunol* **32**, 121–155 (2014).

14. Xu, Y. *et al.* Allogeneic Vγ9Vδ2 T-cell immunotherapy exhibits promising clinical safety and prolongs the survival of patients with late-stage lung or liver cancer. *Cell Mol Immunol* **18**, 427–439 (2021).
15. Di Lorenzo, B. *et al.* Broad Cytotoxic Targeting of Acute Myeloid Leukemia by Polyclonal Delta One T Cells. *Cancer Immunol Res* **7**, 552–558 (2019).
16. Lamb, L. S. *et al.* A combined treatment regimen of MGMT-modified γδ T cells and temozolomide chemotherapy is effective against primary high grade gliomas. *Sci Rep* **11**, 21133 (2021).
17. Tosolini, M. *et al.* Assessment of tumor-infiltrating TCRVγ9Vδ2 γδ lymphocyte abundance by deconvolution of human cancers microarrays. *Oncoimmunology* **6**, e1284723 (2017).
18. Chen, B., Khodadoust, M. S., Liu, C. L., Newman, A. M. & Alizadeh, A. A. Profiling Tumor Infiltrating Immune Cells with CIBERSORT. *Methods Mol Biol* **1711**, 243–259 (2018).
19. Song, L. *et al.* TRUST4: immune repertoire reconstruction from bulk and single-cell RNA-seq data. *Nat Methods* **18**, 627–630 (2021).
20. Susanto, E. *et al.* Modeling SHH-driven medulloblastoma with patient iPS cell-derived neural stem cells. *Proc Natl Acad Sci U S A* **117**, 20127–20138 (2020).
21. Sandén, E. *et al.* Establishment and characterization of an orthotopic patient-derived Group 3 medulloblastoma model for preclinical drug evaluation. *Sci Rep* **7**, 46366 (2017).
22. Harly, C. *et al.* Human γδ T cell sensing of AMPK-dependent metabolic tumor reprogramming through TCR recognition of EphA2. *Sci Immunol* **6**, eaba9010 (2021).
23. Pont, F. *et al.* The gene expression profile of phosphoantigen-specific human γδ T lymphocytes is a blend of αβ T-cell and NK-cell signatures. *Eur J Immunol* **42**, 228–240 (2012).
24. Bockmayr, M. *et al.* Subgroup-specific immune and stromal microenvironment in medulloblastoma. *Oncoimmunology* **7**, e1462430 (2018).
25. Margol, A. S. *et al.* Tumor-associated macrophages in SHH subgroup of medulloblastomas. *Clin Cancer Res* **21**, 1457–1465 (2015).
26. Gentles, A. J. *et al.* The prognostic landscape of genes and infiltrating immune cells across human cancers. *Nat Med* **21**, 938–945 (2015).
27. Meraviglia, S. *et al.* Distinctive features of tumor-infiltrating γδ T lymphocytes in human colorectal cancer. *OncoImmunology* **6**, e1347742 (2017).
28. Zhang, X. M., Tonnelle, C., Lefranc, M. P. & Huck, S. T cell receptor gamma cDNA in human fetal liver and thymus: variable regions of gamma chains are restricted to V gamma I or V9, due to the absence of splicing of the V10 and V11 leader intron. *Eur J Immunol* **24**, 571–578 (1994).
29. Aliseychik, M. *et al.* Dissection of the Human T-Cell Receptor γ Gene Repertoire in the Brain and Peripheral Blood Identifies Age- and Alzheimer's Disease-Associated Clonotype Profiles. *Front. Immunol.* **11**, 497030 (2020).

30. Papadopoulou, M. *et al.* Fetal public Vγ9Vδ2 T cells expand and gain potent cytotoxic functions early after birth. *Proceedings of the National Academy of Sciences* **117**, 18638–18648 (2020).
31. Ivanov, D. P., Coyle, B., Walker, D. A. & Grabowska, A. M. In vitro models of medulloblastoma: Choosing the right tool for the job. *Journal of Biotechnology* **236**, 10–25 (2016).
32. Liu, D. *et al.* Medulloblastoma expresses CD1d and can be targeted for immunotherapy with NKT cells. *Clin Immunol* **149**, 55–64 (2013).
33. Marlin, R. *et al.* Sensing of cell stress by human γδ TCR-dependent recognition of annexin A2. *Proc Natl Acad Sci U S A* **114**, 3163–3168 (2017).
34. Wang, X. *et al.* Diminished cytolytic activity of γδ T cells with reduced DNAM-1 expression in neuroblastoma patients. *Clin Immunol* **203**, 63–71 (2019).
35. Xiao, T. *et al.* Targeting EphA2 in cancer. *Journal of Hematology & Oncology* **13**, 114 (2020).
36. Donovan, L. K. *et al.* Locoregional delivery of CAR T cells to the cerebrospinal fluid for treatment of metastatic medulloblastoma and ependymoma. *Nat Med* **26**, 720–731 (2020).
37. Weishaupt, H. *et al.* Batch-normalization of cerebellar and medulloblastoma gene expression datasets utilizing empirically defined negative control genes. *Bioinformatics* **35**, 3357–3364 (2019).
38. Harly, C. *et al.* Key implication of CD277/butyrophilin-3 (BTN3A) in cellular stress sensing by a major human γδ T-cell subset. *Blood* **120**, 2269–2279 (2012).
39. Cano, C. E. *et al.* BTN2A1, an immune checkpoint targeting Vγ9Vδ2 T cell cytotoxicity against malignant cells. *Cell Reports* **36**, (2021).
40. Bukowski, J. F. *et al.* V gamma 2V delta 2 TCR-dependent recognition of non-peptide antigens and Daudi cells analyzed by TCR gene transfer. *The Journal of Immunology* **154**, 998–1006 (1995).
41. Payne, K. K. *et al.* BTN3A1 governs antitumor responses by coordinating αβ and γδ T cells. *Science* **369**, 942–949 (2020).
42. Dietrich, J. Neurotoxicity of Cancer Therapies. *CONTINUUM: Lifelong Learning in Neurology* **26**, 1646 (2020).
43. Schmahmann, J. D. The cerebellum and cognition. *Neurosci Lett* **688**, 62–75 (2019).
44. Heipertz, E. L. *et al.* Current Perspectives on 'Off-The-Shelf' Allogeneic NK and CAR-NK Cell Therapies. *Front Immunol* **12**, 732135 (2021).
45. Adoptive T cell therapy: Boosting the immune system to fight cancer. *Seminars in Immunology* **49**, 101437 (2020).
46. Costa, G. P., Mensurado, S. & Silva-Santos, B. Therapeutic avenues for γδ T cells in cancer. *J Immunother Cancer* **11**, e007955 (2023).
47. Gorsi, H. S. *et al.* Nivolumab in the Treatment of Recurrent or Refractory Pediatric Brain Tumors: A Single Institutional Experience. *Journal of Pediatric Hematology/Oncology* **41**, e235 (2019).

48. Guo, X., Chang, M., Wang, Y., Xing, B. & Ma, W. B7-H3 in Brain Malignancies: Immunology and Immunotherapy. *Int J Biol Sci* **19**, 3762–3780 (2023).
49. Majzner, R. G. *et al.* CAR T Cells Targeting B7-H3, a Pan-Cancer Antigen, Demonstrate Potent Preclinical Activity Against Pediatric Solid Tumors and Brain Tumors. *Clin Cancer Res* **25**, 2560–2574 (2019).
50. Kramer, K. *et al.* Phase 1 study of intraventricular 131I-omburtamab targeting B7H3 (CD276)-expressing CNS malignancies. *Journal of Hematology & Oncology* **15**, 165 (2022).
51. Lu, H. *et al.* B7-H3 confers resistance to Vγ9Vδ2 T cell-mediated cytotoxicity in human colon cancer cells via the STAT3/ULBP2 axis. *Cancer Immunol Immunother* **70**, 1213–1226 (2021).
52. Jiang, Z.-M. *et al.* Development of genetically engineered iNKT cells expressing TCRs specific for the M. tuberculosis 38-kDa antigen. *Journal of Translational Medicine* **13**, 141 (2015).
53. Rietkötter, E. *et al.* Zoledronic acid inhibits macrophage/microglia-assisted breast cancer cell invasion. *Oncotarget* **4**, 1449–1460 (2013).
54. Morris, E. C., Neelapu, S. S., Giavridis, T. & Sadelain, M. Cytokine release syndrome and associated neurotoxicity in cancer immunotherapy. *Nat Rev Immunol* **22**, 85–96 (2022).

Figure legends

Figure 1: γδT cells abundance in MB tumors. (**A**) Immune cell infiltration and abundance in MB (n=76) versus normal fetal (n=5) and adult (n=4) cerebellum samples. (**B**) Immune cell infiltration and abundance in MB subgroups (WNT-MB n=70; SHH-MB n=222; Grp3-MB n=143; Grp4-MB n=325). (**C**) γδT and (**D**) αβT cells abundance across MB subgroups. Statistical analysis was performed using one-way ANOVA followed by Dunnett tests to correct for WNT-MB, SHH-MB, and Grp3-MB vs Grp4-MB (**P = 0.0037; ****P < 0.0001). (**E**) γδT abundance across MB subtypes. (**F**) Overall survival of patients grouped according to high or low abundance of γδT cells in MB all subgroups (1st and last quartile, n=306 per group). Significance was determined by log-rank test – nonsignificant differences are not displayed in the figure.

Figure 2: Infiltrated γδTCR repertoire and differentiation state (A) TCR *TRGV* gene repertoire repartition (n=52 γδT cells, in 24 patients, GSE156053). (**B**) *TRGV* and *TRGJ* gene expression repartition across MB subgroups. (**C**) Relative frequency of the Vγ chain CDR3 across MB subgroups. (**D**) Normalization of 30 gene expression of the identified αβT and γδT cells representative of five T cell differentiation state (n = n=56 αβT cells and n=52 γδT cells). (**E**) Signature score of each T cell differentiation state cluster.

Figure 3: γδTCR, and γδT co-receptor ligand expression by MB cell lines. Fold change of MFI (Median of fluorescence) of expression of γδTCR, and γδT co-receptor ligands on seven MB cell lines

compared to corresponding isotype controls, acquired by flow cytometry (dashed line =1, threshold of expression).

Figure 4: Vγ9Vδ1 TCR recognition of EphA2-positive MB cells. Analysis by flow cytometry of CD69 surface expression on Jurkat JRT3 MAU (Vγ9Vδ1 TCR positive) after a 4 h-co-culture (E/T ratio 1:1) with (**A**) Neuroepithelial Stem cells (NES) and MB cell lines, or (**D**) Grp3 PDX cells. n= 3 independent experiments. Statistical analysis was performed using one-way ANOVA followed by Dunnett tests to correct for multiplicity (**P* < 0.05; ****P* = 0.0001; *****P* < 0.0001). (**B**) Fold change of MFI (Median of fluorescence) of EphA2 expression on NES. n= 3 independent experiments. Statistical analysis was performed using Unpaired t-test (**P* < 0.05). (**C**) *EPHA2* mRNA expression in human MB subgroups versus normal human cerebellum (crbl). Statistical analysis was performed using one-way ANOVA followed by Dunnett tests to correct for multiplicity (**P* < 0.05) – nonsignificant differences are not displayed in the figure.

Figure 5: Vγ9Vδ2 TCR recognition of zoledronate-treated MB cells. (A) Schematic of the action of zoledronate in the cholesterol synthesis pathway leading to the activation of the Vγ9Vδ2 TCR via the BTN3A1/2A1 complex. (B) Percentage of total γδT cells in the ex vivo expanded population and percentage of the different γδT cell subsets assessed by flow cytometry. n=12 donors (C) Analysis by flow cytometry of CD107a expression on ex vivo-expanded human Vδ2T cells after 4 h of co-culture Neuroepithelial Stem cells (NES) and MB cell lines treated with 0 or 10 µM of zol (E/T ratio 1:1). n = 4-6 donors. (**D**)-(**G**) Analysis of cytotoxicity by LDH release in the supernatant, after 8 h-co-culture with ex vivo expanded γδT cells, by (**D**) SHH-MB cell lines grown in monolayer (m) or spheroid (sph), treated with 0 or 20 µM of zol; (**E**) by SHH-MB cell lines grown in monolayer (m), treated with 0 or 20 µM of zol with or without pre-conditioning with NKG2D blocking antibody (10µg/ml); (**F**) by Grp3- and Grp4-MB grown in suspension (s), treated with 0 or 50 µM of zol; (**G**) by differentiated neurons and NES grown monolayer (m) or spheroid (sph), treated with 0 or 50 µM of zol. n = 3-6 donors; statistical analysis was performed using two-way ANOVA followed by (C) Dunnett, (D) Tukey (E)- (G) Sidak tests to correct for multiplicity (**P* < 0.05; ***P* < 0.005; ****P* = 0.0001; *****P* < 0.0001) – nonsignificant differences are not displayed in the figure.

Figure 1

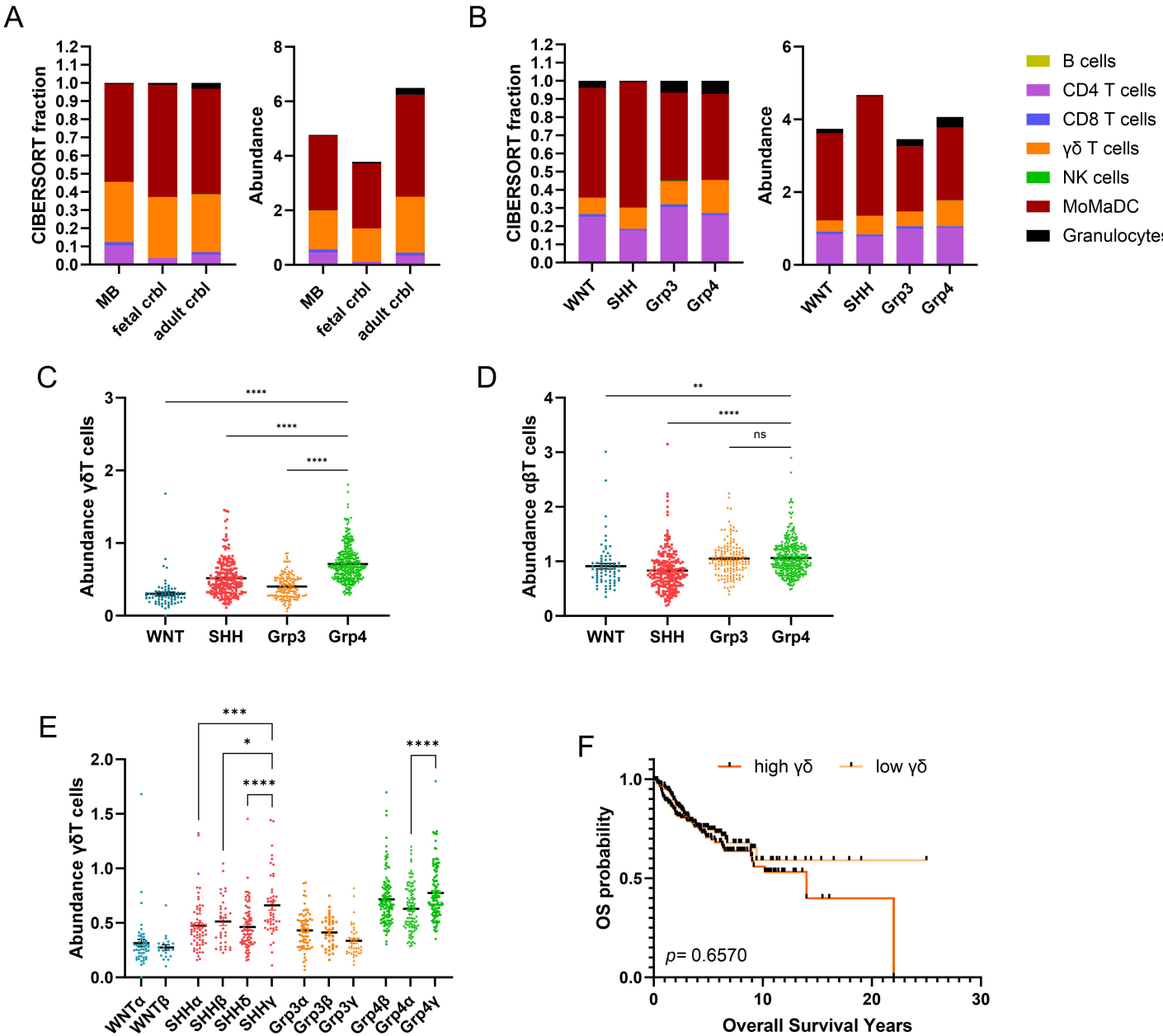
A
CIBERSORT fraction
Abundance
MB
fetal crbl
adult crbl
B
WNT
SHH
Grp3
Grp4
B cells
CD4 T cells
CD8 T cells
γδ T cells
NK cells
MoMaDC
Granulocytes
C
Abundance γδT cells
****
D
Abundance αβT cells
**
ns
E
Abundance γδT cells
***
*
WNTα
WNTβ
SHHα
SHHβ
SHHδ
SHHγ
Grp3α
Grp3β
Grp3γ
Grp4β
Grp4α
Grp4γ
F
high γδ
low γδ
OS probability
p= 0.6570
Overall Survival Years

Figure 2

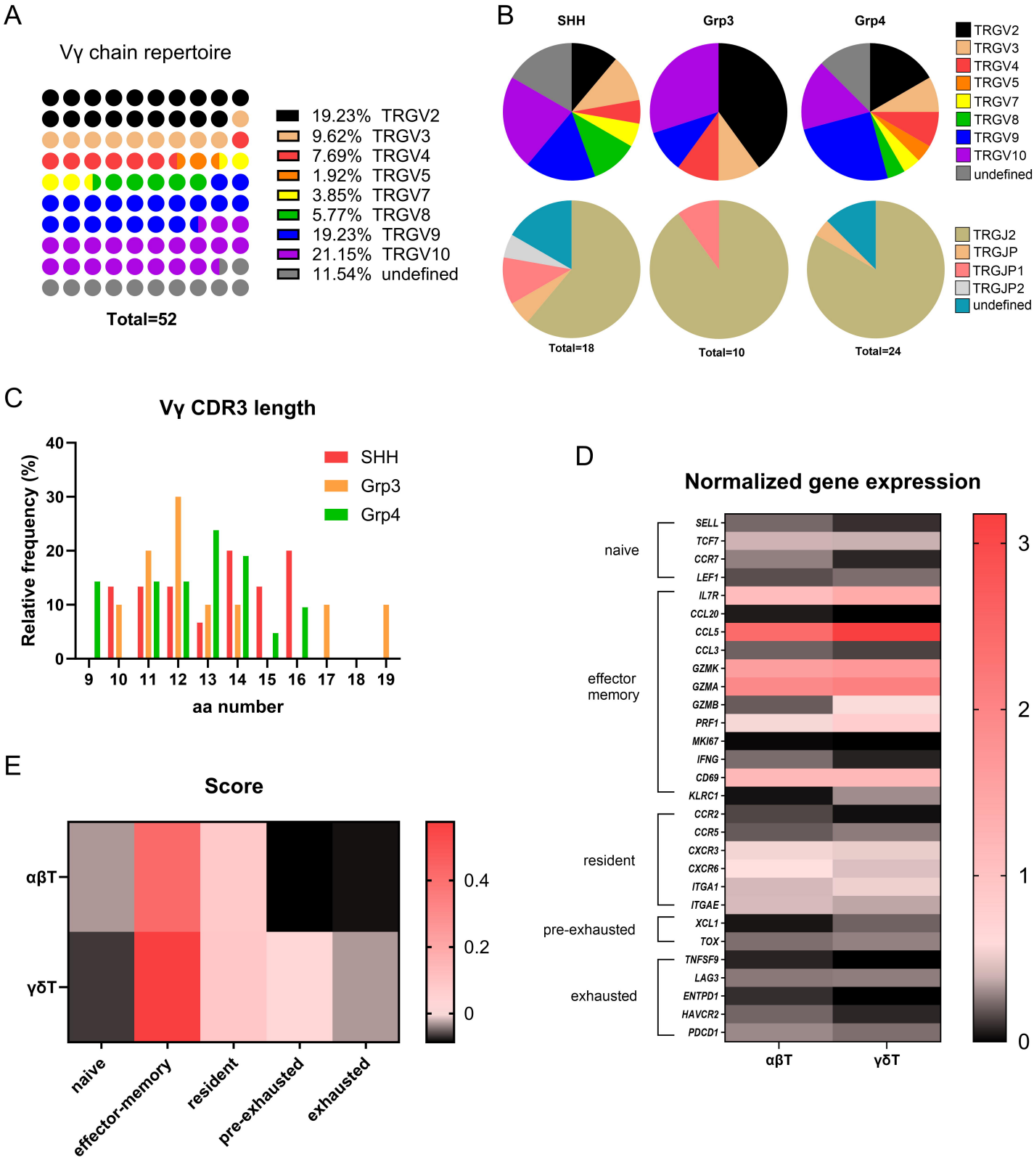
A
Vγ chain repertoire
19.23% TRGV2
9.62% TRGV3
7.69% TRGV4
1.92% TRGV5
3.85% TRGV7
5.77% TRGV8
19.23% TRGV9
21.15% TRGV10
11.54% undefined
Total=52
B
SHH
Grp3
Grp4
TRGV2
TRGV3
TRGV4
TRGV5
TRGV7
TRGV8
TRGV9
TRGV10
undefined
TRGJ2
TRGJP
TRGJP1
TRGJP2
undefined
Total=18
Total=10
Total=24
C
Vγ CDR3 length
Relative frequency (%)
SHH
Grp3
Grp4
aa number
D
Normalized gene expression
naive
effector memory
resident
pre-exhausted
exhausted
SELL
TCF7
CCR7
LEF1
IL7R
CCL20
CCL5
CCL3
GZMK
GZMA
GZMB
PRF1
MKI67
IFNG
CD69
KLRC1
CCR2
CCR5
CXCR3
CXCR6
ITGA1
ITGAE
XCL1
TOX
TNFSF9
LAG3
ENTPD1
HAVCR2
PDCD1
αβT
γδT
E
Score
αβT
γδT
naive
effector-memory
resident
pre-exhausted
exhausted

Figure 3

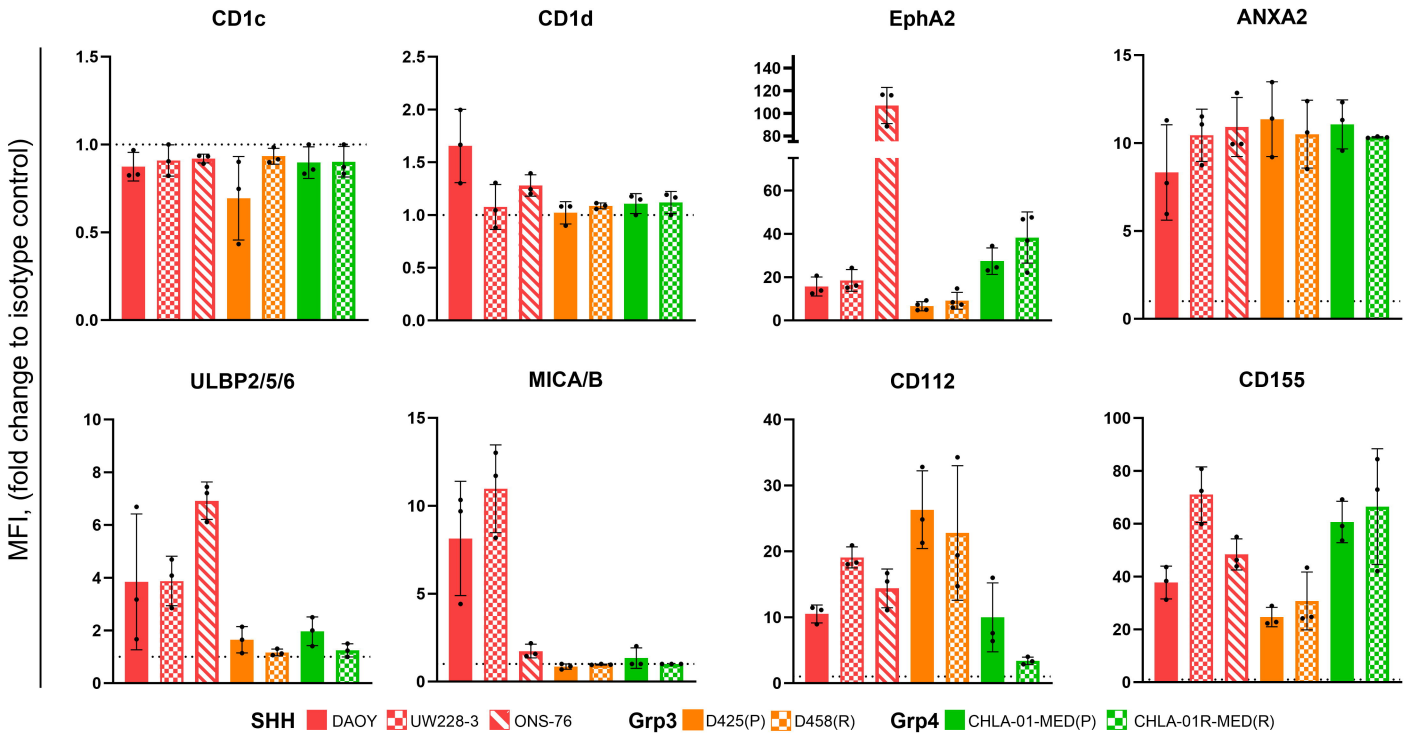
CD1c
CD1d
EphA2
ANXA2
ULBP2/5/6
MICA/B
CD112
CD155
MFI, (fold change to isotype control)
SHH
DAOY
UW228-3
ONS-76
Grp3
D425(P)
D458(R)
Grp4
CHLA-01-MED(P)
CHLA-01R-MED(R)

Figure 4

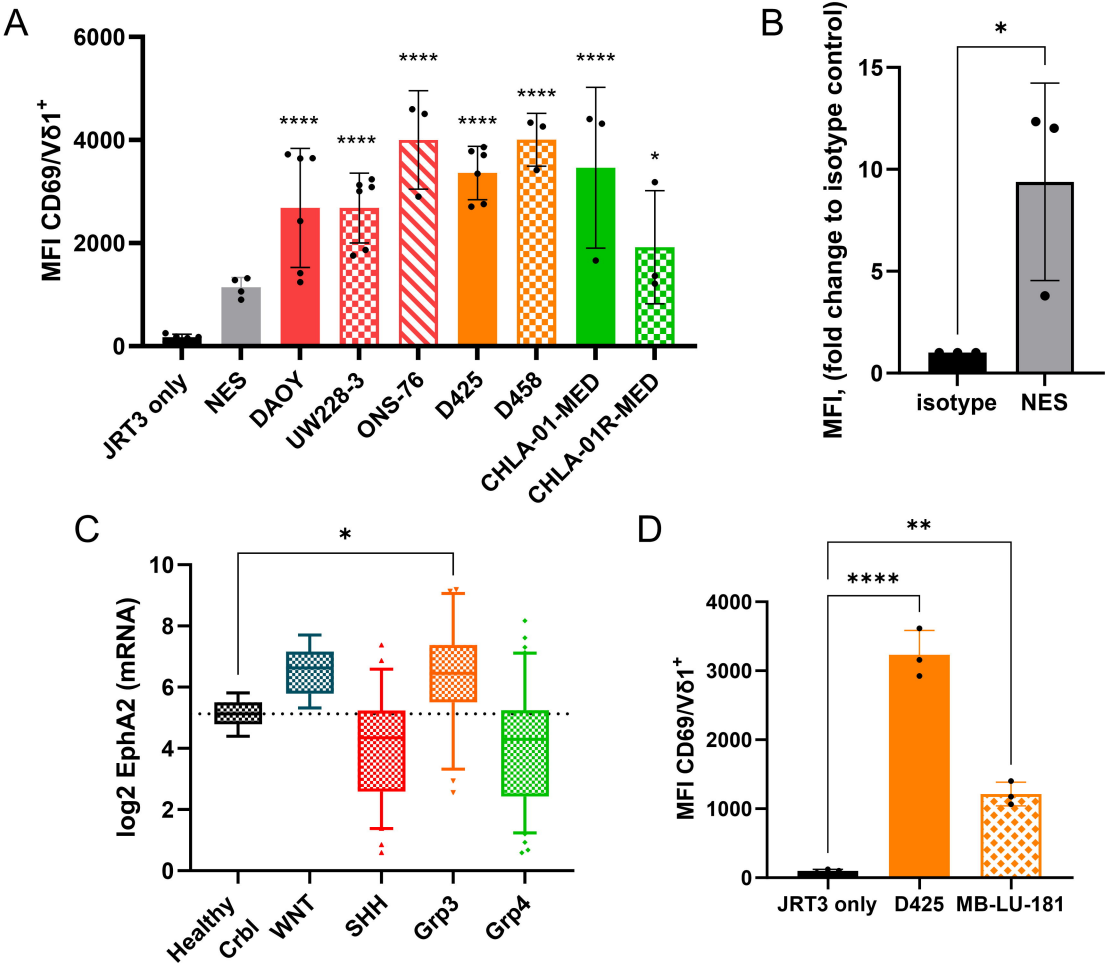
A
MFI CD69/Vδ1+
6000
4000
2000
0
****
****
****
****
****
*
JRT3 only
NES
DAOY
UW228-3
ONS-76
D425
D458
CHLA-01-MED
CHLA-01R-MED
B
MFI, (fold change to isotype control)
15
10
5
0
*
isotype
NES
C
log2 EphA2 (mRNA)
10
8
6
4
2
0
*
Healthy
Crbl
WNT
SHH
Grp3
Grp4
D
MFI CD69/Vδ1+
4000
3000
2000
1000
0
**
****
JRT3 only
D425
MB-LU-181

Figure 5

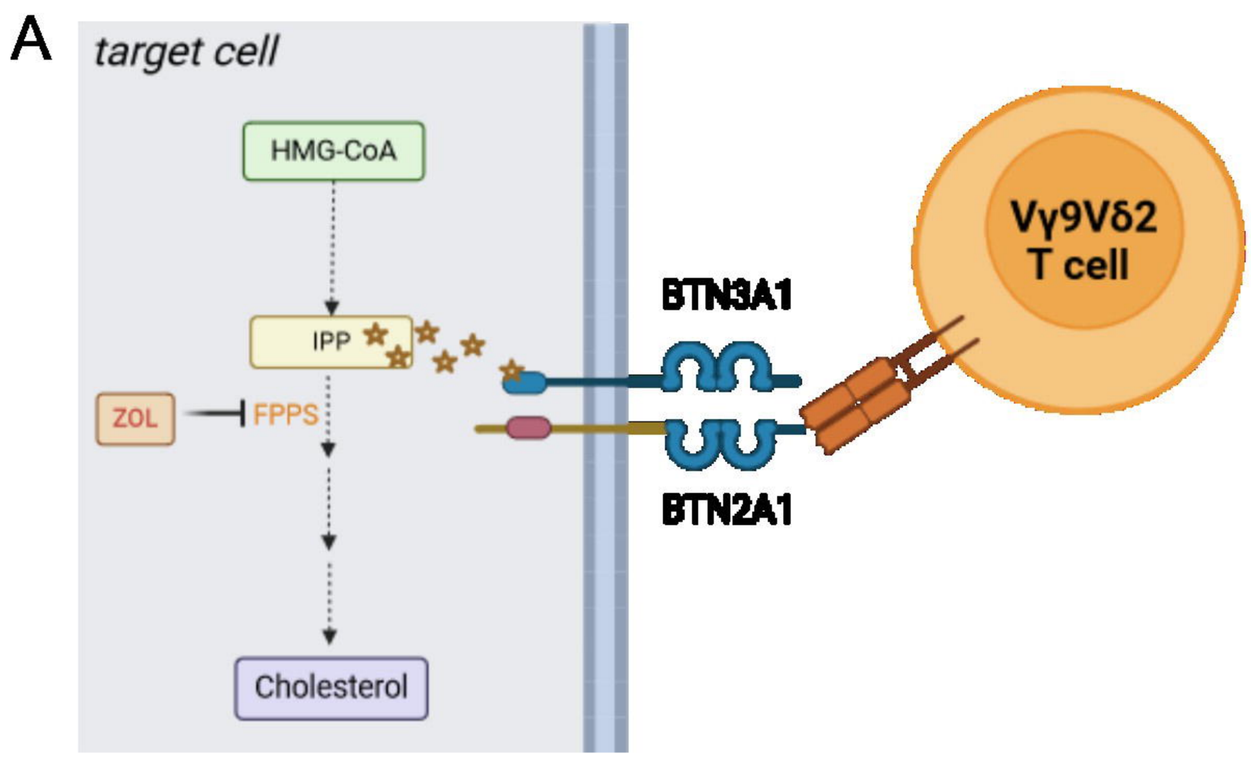
A
target cell
HMG-CoA
IPP
ZOL
FPPS
Cholesterol
BTN3A1
BTN2A1
Vγ9Vδ2
T cell

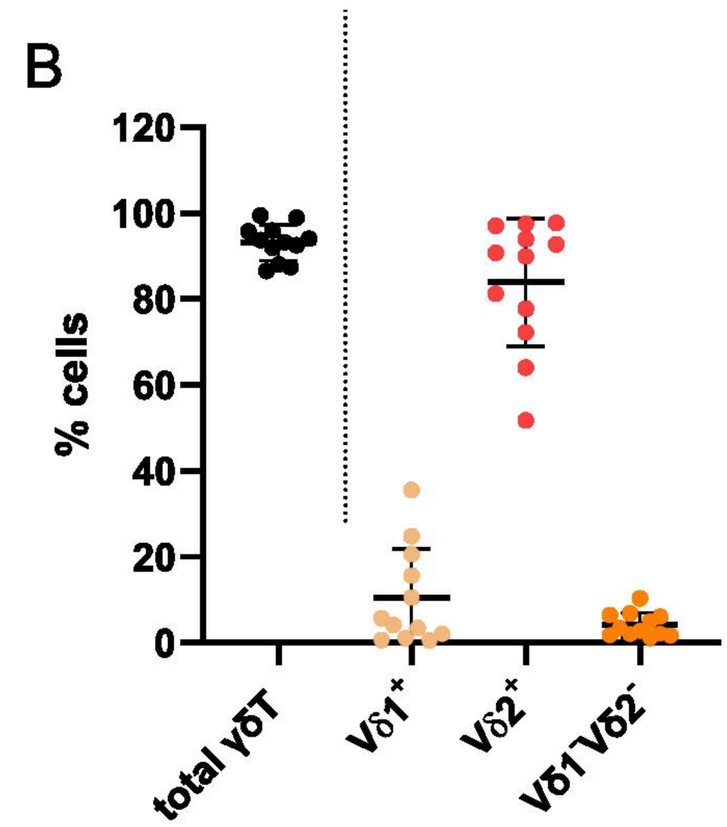
B
% cells
120
100
80
60
40
20
0
total γδT
Vδ1+
Vδ2+
Vδ1-Vδ2-

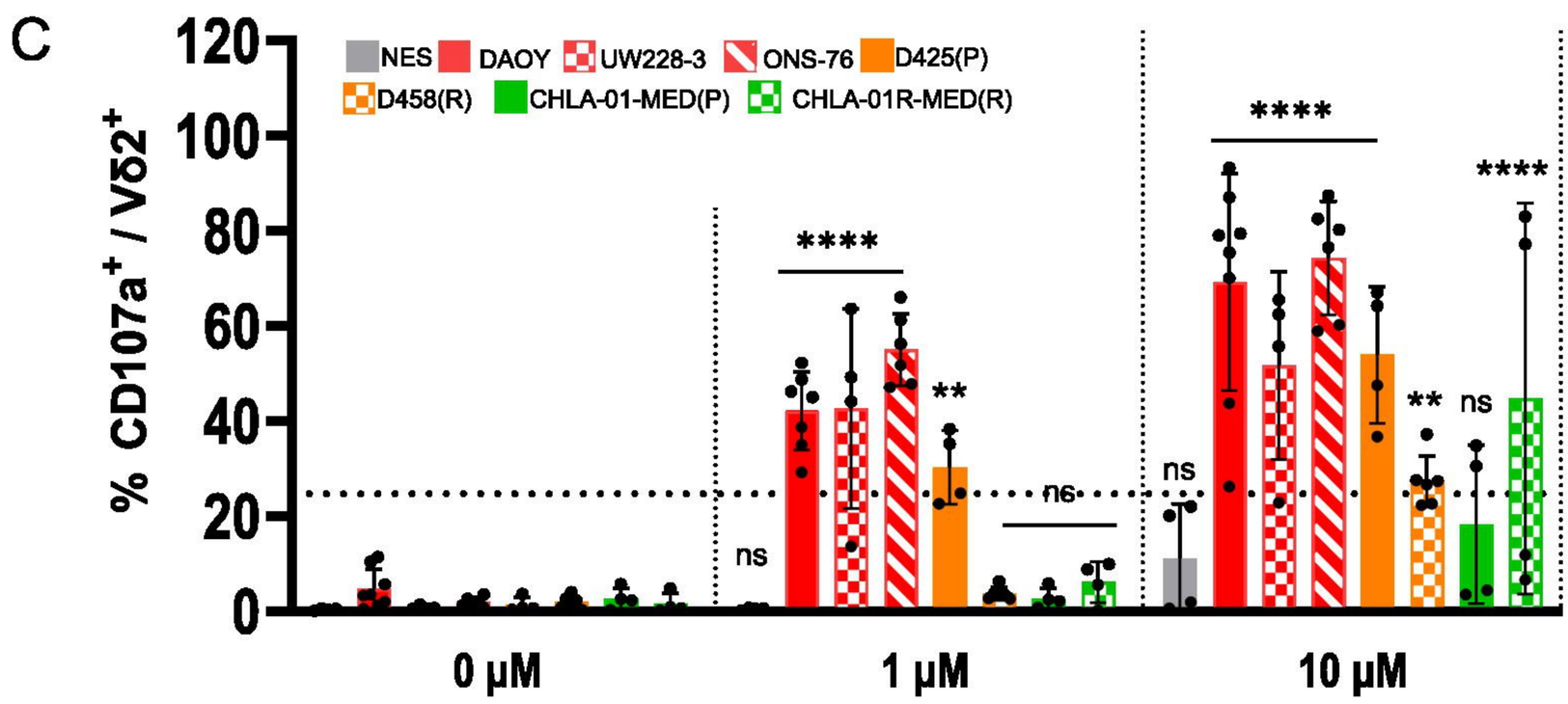
C
% CD107a+ / Vδ2+
NES
DAOY
UW228-3
ONS-76
D425(P)
D458(R)
CHLA-01-MED(P)
CHLA-01R-MED(R)
****
**
ns
0 μM
1 μM
10 μM

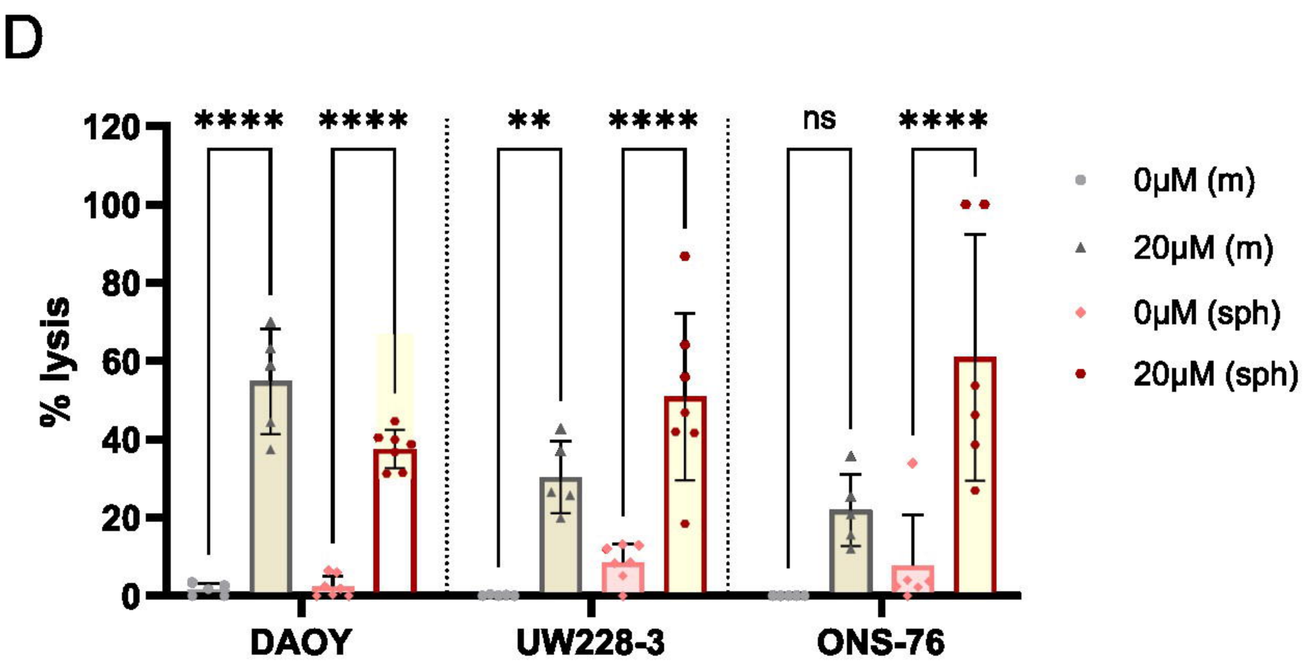
D
% lysis
****
**
ns
DAOY
UW228-3
ONS-76
0μM (m)
20μM (m)
0μM (sph)
20μM (sph)

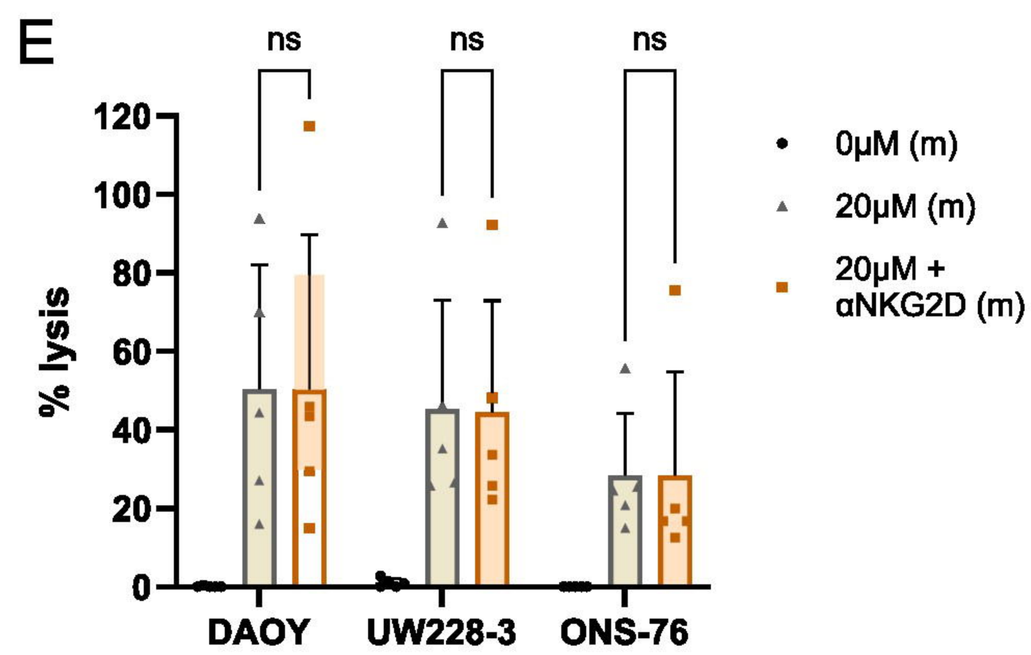
E
% lysis
ns
DAOY
UW228-3
ONS-76
0μM (m)
20μM (m)
20μM + αNKG2D (m)

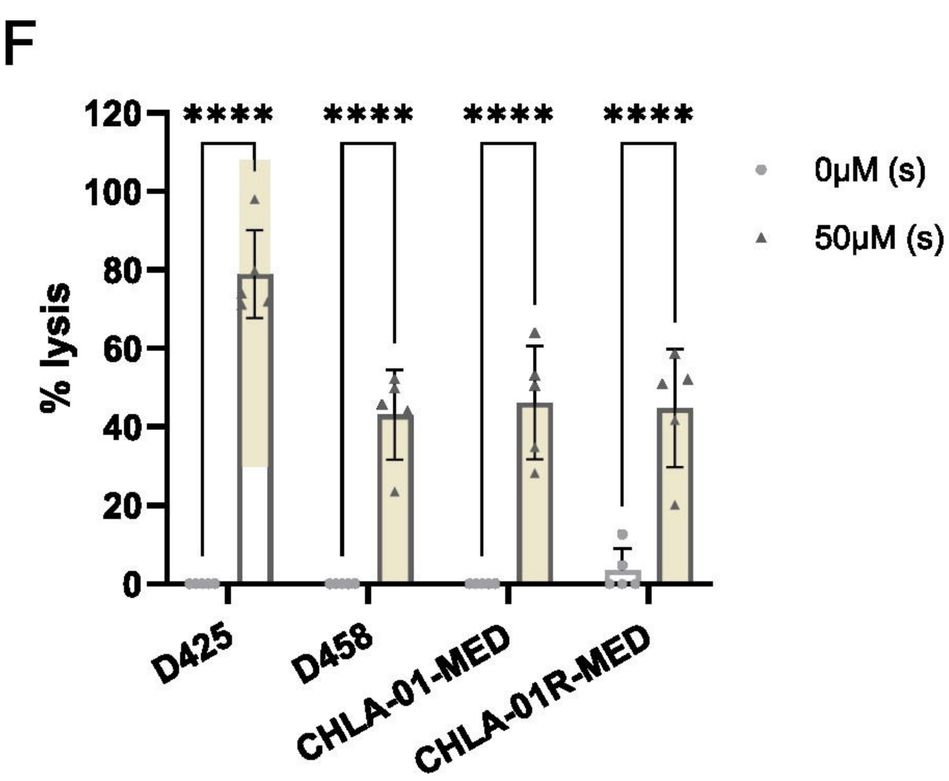
F
% lysis
****
D425
D458
CHLA-01-MED
CHLA-01R-MED
0μM (s)
50μM (s)

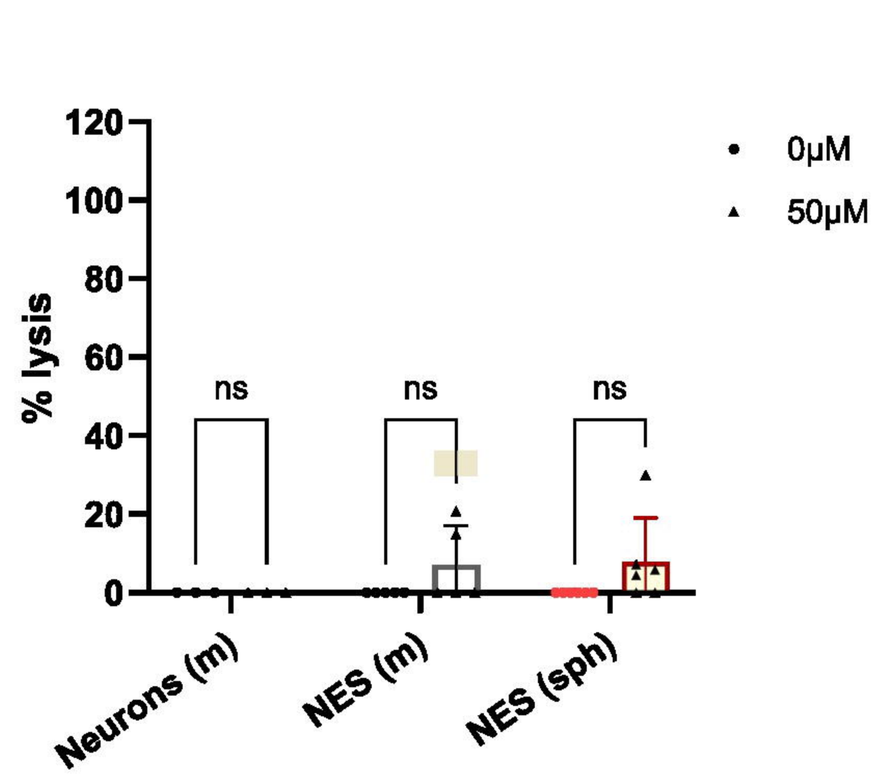
G
% lysis
ns
Neurons (m)
NES (m)
NES (sph)
0μM
50μM